Atmos. Chem. Phys. Discuss., 14, 14351–14397, 2014
www.atmos-chem-phys-discuss.net/14/14351/2014/
doi:10.5194/acpd-14-14351-2014

Atmospheric Chemistry and Physics Discussions
Open Access

Recent trends in aerosol optical properties derived from AERONET measurements

J. Li[1,2], B. E. Carlson[1], O. Dubovik[3], and A. A. Lacis[1]

[1]Goddard Institute for Space Studies, New York, NY, USA
[2]Department of Applied Physics and Applied Math, Columbia University, New York, NY, USA
[3]French National Centre for Scientific Research, University Lille 1, France

Received: 14 March 2014 – Accepted: 16 May 2014 – Published: 3 June 2014

Correspondence to: J. Li (jl2862@columbia.edu)

Published by Copernicus Publications on behalf of the European Geosciences Union.

Abstract

The Aerosol Robotic Network (AERONET) has been providing high-quality retrievals of aerosol optical properties from the surface at worldwide locations for more than a decade. Many sites have continuous and consistent records for more than 10 years, which enables the investigation of long-term trends of aerosol properties at these locations. In this study, we present trend analysis of AERONET data at 63 selected locations. In addition to commonly studied parameters such as Aerosol Optical Depth (AOD) and Ångström Exponent (AE), we also focus on Absorption Aerosol Optical Depth (ABS), Scattering Optical Depth (SCT), Single Scattering Albedo (SSA) and the Absorption Ångström Exponent (AAE). Two statistical methods are used to detect and estimate the trend: Mann–Kendall test associated with Sen's slope and linear least square fitting. Their results agree well in terms of the significance of the trend for the majority of the cases. The results indicate that Europe and North America experienced a uniform decrease in AOD and SCT, while significant ($>90\,\%$) increases of these two parameters are found for Kanpur, India. Most of European and North American sites also show negative trends for ABS, as well as three East Asian stations. The reduction in ABS results in positive SSA trends for these locations. The increase of SCT also leads to a positive SSA trend for Kanpur. Negative SSA trends are mostly found over South America, Australia and a few West European stations, which are mainly attributed to the increase of absorption. Fewer stations are found with significant trends for AE and AAE. In general, the trends do not exhibit obvious seasonality for the majority of the parameters and stations.

1 Introduction

Atmospheric aerosols have been recognized as an important climate forcing agent (Charlson et al., 1992) and play a critical role in global climate change (IPCC, 2013). The climate effect of aerosols is determined by their optical properties, including scat-

ACPD
14, 14351–14397, 2014

tering and absorption. Changes in these properties will thus alter the radiative forcing of aerosols. Therefore, understanding the variability in these optical properties is essential in quantifying their role in recent climate variability and climate change. Among the aerosol variabilities at different time scales, long-term trends are of particular interest, because they help us understand the global and regional cycling of different aerosol species of both natural and anthropogenic origin, as well as validate emission inventories and the representation of aerosols in climate models. Aerosol trends are also critical in resolving the change of surface radiation balance over the past few decades, such as global brightening found over multiple locations in Europe and North America (Wild et al., 2005, 2009).

Previously, many studies have investigated long-term trends in aerosol loading and related parameters using satellite or ground-based remote sensing data or in-situ measurements. Mishchenko et al. (2007) reported a global decline in AOD since the 1990's found in AVHRR retrievals. Zhang and Reid (2010) studied regional AOD trends using MODIS and MISR over water product and revealed regional differences in the trends. Xia (2011) analyzed AOD trends using AERONET data at 79 locations and found significant decreases over North America and Europe. Other studies analyzed trends in visibility as an aerosol proxy (e.g., Mahowald et al., 2007; Wang et al., 2009; Stjern et al., 2011), or inferred aerosol trends from solar radiation (e.g., Wild, 2009, 2012). Most of the above studies focused on the primary aerosol loading indicator which is the optical depth. A few also involved Ångström Exponent. However, the trends in other aerosol properties, in particular, aerosol absorption, scattering and single scattering albedo, remain less well known, partly attributed to the difficulty in retrieving these variables using remote sensing techniques. Yet, aerosol absorption and single scattering albedo are equally, or even more important in determining aerosol forcing. Changes in these quantities impact heavily on both aerosol direct effect and aerosol-cloud interaction. Recently, Collaud Coen et al. (2013) analyzed long-term trends in aerosol scattering and absorption coefficients using in-situ measurements at US and European locations. Their study indicated significant reduction in scattering coefficients for

ACPD
14, 14351–14397, 2014

both US and Europe, with less significant reduction in absorption coefficients. These results both improve our understanding of changes in aerosol optical properties and provide an assessment of emission reduction policies. Atmosphere inversion products from AERONET (Holben et al., 1998; Dubovik and King, 2000, Dubovik et al. 2006) involve column retrievals of aerosol scattering and absorption, which complement in-situ measurements in providing column optical information. In addition, the AERONET network is much more extensive, covering many important aerosol source regions such as Africa, South America and Asia. As a result, an analysis of long-term trends revealed by AERONET measurements is desirable to better understand the recent changes in aerosol properties over worldwide locations.

A major difficulty in using AERONET inversion products for trend analysis is the uncertainty of the measurements. The accuracy of the retrievals was analyzed in extensive sensitivity studies by Dubovik et al. (2000). Based on the results of these studies Dubovik at al. (2002) recommended a set of criteria for selecting the high quality retrieval of all aerosol parameters including aerosol absorption. These recommendations were adapted as part of quality assurance criteria applied to produce quality-assured Level 2.0 inversion product (Holben et al., 2006). One of the adapted criteria excludes all cases with AOD < 0.4 because Dubovik et al. (2000) indicated significant decrease in accuracy of aerosol parameters with the decrease of aerosol optical thickness. For example, the accuracy of SSA retrieval was dropping from 0.03 to 0.05–0.07 for AOD values of 0.2 and less. However, the observations with AOD < 0.4 actually represent bulk of the data for many stations. As a result, due to this data screening, very few stations have long-term consistent Level 2.0 data records and we need to rely on Level 1.5 data. Moreover, with gaps even in Level 1.5 records and non-normal distribution of some parameters, caution must be taken when using statistical methods to estimate the magnitude and significance of trends.

In this study, we use AERONET inversion products from 63 selected stations to examine trends in major aerosol optical properties, including optical depth, (AOD), Ångström exponent, (AE), absorption optical depth (ABS), scattering optical depth

ACPD
14, 14351–14397, 2014

(SCT), single scattering albedo (SSA) and absorption Ångström exponent (AAE). Although Level 1.5 data are used for the majority of the stations, comparison at the few stations with sufficient Level 2.0 data indicates consistency of the trends between these two data levels. Also, both Mann–Kendall test as well as linear least square fitting are used to detect the trends in order to improve the robustness of the results.

The paper is organized as follows: Sect. 2 introduces the AERONET inversion products and describes data selection criteria. Section 3 introduces the analysis techniques with some examples. Trends for the six parameters are presented in Sect. 4. Some discussions of the results are given in Sect. 5. And Sect. 6 concludes with a summary of the major findings.

2 AERONET data

The aerosol parameters used in the trend study include aerosol extinction optical depth (AOD), absorption optical depth (ABS), scattering optical depth calculated by subtracting ABS from AOD, single scattering albedo (SSA), all at 440 nm, and Ångström Exponent (AE) for the 440 nm and 870 nm wavelength interval and absorption Ångström Exponent (AAE) for the 440 nm and 870 nm wavelength interval. The data are obtained from the version 2 AERONET inversion product using almucantar retrievals (Holben et al., 1998; Dubovik and King, 2000, Dubovik et al. 2006). Ideally, one prefers to use Level 2.0 data that are quality assured. However, the AOD threshold of 0.4 applied to the data, as required by the quality assurance criteria (Holben et al., 2006), eliminates the bulk of the data, especially for stations in North America, South America, and Europe where aerosol loading is typically low. Figure 1 shows the distribution of AERONET AOD for the globe and five regions, using the stations selected for this study as described in the next paragraph. The small panel in the upper right corner of each larger panel shows the enlarged distribution for the [0, 0.5] AOD interval, and the threshold value of 0.4 is denoted by black dashed lines. We can clearly see that the AOD > 0.4 portion only captures the tail of the AOD distribution, while the bulk of the

ACPD
14, 14351–14397, 2014

data fall between 0 and 0.4. Even for Africa and Asia, where AOD are, in general, larger, the 0.4 cut-off will still eliminate roughly 75 % of the data. Since AOD and AE are from the direct-beam product and not subject to the AOD > 0.4 screening for Level 2 product we use the Level 2 AOD and AE parameters, while the Level 1.5 cloud screened (Smirnov et al., 2000) inversion product is used for the ABS, SSA and AAE parameters, to ensure a greater spatial and temporal coverage is used for most stations. This approach is appropriate because while the sensitivity analysis by Dubovik et al. (2000) suggested a drop in the accuracy of the aerosol retrievals at lower AODs they did not find any biases. Moreover, later analysis by Kaufman et al. (2002) did not find any biases in the retrieved absorption even at very low AODs. Moreover, AERONET Level 1.5 or lower products have been frequently used in many other applications where the increased spatial coverage is desirable, such as the validation of satellite retrieval products (Remer et al., 2002; Kahn et al., 2005; Christopher et al., 2008; Cheng et al., 2012) and the study of aerosol compositions (Omar et al., 2005; Prasad and Singh, 2007; Mallet et al., 2013). Nonetheless, due to limitations in data quality, some outliers still exist in Level 1.5 data, especially for the SSA parameter. We therefore screen the data by removing any cases for which SSA is below 0.5.

For the purpose of our long-term trend study, we select stations purely based on the availability of an extensive data record. Specifically, we first calculate monthly medians of the parameters using all-point measurements. The reason of using the median instead of the mean is that many optical parameters such as optical depth do not follow a normal distribution, in which case the median is a better representation than the mean. A monthly median is considered valid only if there are more than 5 point measurements for that month. To ensure a continuous time series, we require the data record to have at least 6 years of measurements with no less than 9 monthly data points for each year during the 2000 to 2013 period. A total of 63 stations are selected, only 4 of these stations have qualified Level 2.0 inversion data, therefore the Level 1.5 inversion products are used for the remainder of the 59 stations. The geographic locations

ACPD
14, 14351–14397, 2014

of the selected stations are shown in Fig. 2. The first four columns of Table 1 list the name, location and number of available monthly medians for each station.

3 Trend analysis

Detecting trends in time series data is a non-trivial task, especially when many of the parameters are not normally distributed and autocorrelation associated with seasonality usually exists in the record. To determine and estimate annual trends, a two-step approach is taken here. First, we apply a 12 month running mean to the de-seasonalized data (by removing multi-year averaged seasonal cycle) to manually observe the underlying smoothed structure. Next, two statistical methods – seasonal Mann–Kendall (MK) test associated with Sen's slope and linear least square fitting of the de-seasonalized data, are used to further test and estimate the trends. Moreover, we also estimate the trend using the MK and least square methods for each season in order to examine whether there is obvious seasonality in the trends. The two trend analysis techniques are described in the following two subsections.

3.1 Mann–Kendall test and Sen's slope

The Mann–Kendall statistical test (Mann, 1945; Kendall, 1975) is a non-parametric test to identify whether monotonic trends exist in a time series. The advantage of the non-parametric statistical tests over the parametric tests, such as the t test, is that the non-parametric tests are more suitable for non-normally distributed, censored, and missing data, which are frequently encountered in the AERONET data record. However, many time series of aerosol parameters may frequently display statistically significant serial correlation, especially those associated with seasonal variability. In such cases, the existence of serial correlation will increase the probability that the MK test detects a significant trend (von Storch, 1995; Yue et al., 2002; Zhang and Zwiers, 2004). It is therefore necessary to "pre-whiten" the time series by eliminating the influence of

ACPD
14, 14351–14397, 2014

AR(1) serial correlation before performing the test. Yue et al. (2002) indicate that directly removing the AR(1) component from the raw time series also removes part of the magnitude of the trend and proposed a pre-whitening scheme by first removing the linear trend form the time series by

$$X'_t = X_t - T_t = X_t - bt \tag{1}$$

where b is the slope of the trend estimated using Sen's method (Sen, 1968), and then removing the AR(1) component from X'_t by

$$Y'_t = X'_t - r_1 X'_{t-1} \tag{2}$$

r_1 is lag-1 autocorrelation, and finally adding the trend back by

$$Y_t = Y'_t + T_t \tag{3}$$

The blended time series Y_t preserves the true trend but is no longer influenced by the effect of autocorrelation. Furthermore, Hirsch et al. (1982, 1984) extended the MK test to take seasonality into account, and estimated annual trend as the median of seasonal trends. Here we adopt the Yue et al. (2002) pre-whitening scheme and perform the Seasonal MK test on the pre-whitened times series Y_t. Two-tailed tests at both 95 % and 90 % significance level were applied to test either an upward or downward trend.

To estimate the true slope b of the trend, we use the non-parametric procedure developed by Sen (1968) as follows:

$$b = \text{Median}\left(\frac{X_i - X_j}{i - j}\right) \quad \forall j < i \tag{4}$$

A 90 % significance level is applied to calculate the upper and lower limits of the confidence interval of the slope. Compared to other slope estimators such as linear regression coefficient, the Sen's slope is much less sensitive to outliers, which is particularly suitable for Level 1.5 data in which outliers occasionally appear.

ACPD
14, 14351–14397, 2014

3.2 Linear least square fitting

Linear trends and their significance level are also estimated using the method by Weatherhead et al. (1998). The data time series is modeled by fitting the following relationship with a least square approximation:

$$Y_T = Y_0 + bt + N_t \tag{5}$$

Y_t is the de-seasonalized monthly median time series, b is the linear trend, Y_0 is the offset at the start of the time series, and N_t is the noise term. The noise term N_t is further modeled as an AR(1) process:

$$N_t = \phi N_{t-1} + \varepsilon_t \tag{6}$$

Weatherhead et al. (1998) suggested that the standard deviation of the yearly trend σ_b can be estimated as

$$\sigma_b \approx \frac{\sigma_n}{n^{3/2}} \sqrt{\frac{1+\phi}{1-\phi}} \tag{7}$$

where ϕ is the standard deviation of N_t, and n equals the total number of years in the series. Weatherhead et al. (1998) also found that if $|b/\sigma_b| > 2$, the trend is significant at 95 % significance level. And 90 % level is found for $|b/\sigma_b| > 1.65$ (Hsu et al., 2012). In large number of application, the least squares approach is based on the Gaussian distribution of uncertainties. However, a number of studies have pointed out that this assumption is often not appropriate for the analysis of some properties derived in remote sensing applications. For example, Ignatov et al. (2000) suggested using the lognormal distribution as a reference for reporting aerosol optical depth statistics. Moreover, Dubovik and King (2000) and earlier Dubovik et al. (1995) have pointed to the importance of using log-normal distribution as a noise assumption in statistically optimized fitting of positively defined physical characteristics. Indeed, the curve of the

ACPD
14, 14351–14397, 2014

normal distribution is symmetrical and the assumption of a normal probability density distribution necessarily implies the possibility of negative results arising even in the case of physically nonnegative values (e.g. intensities). For nonnegative characteristics, this assumption is clearly more reasonable. First, log-normally distributed values are positively-defined and a number of theoretical and experimental reasons show that for positively defined characteristics the log-normal curve (multiplicative errors, Edie et al., 1971) is closer to reality than normal noise (additive errors, a statistical discussion can be found in Tarantola, 1987). Therefore in the present study, the least squares fitting for AOD, ABS and SCT is performed on the logarithm of the data.

3.3 Analysis example

Here we show an example of the trends observed by running mean, and estimated using MK/Sen's slope and least squares fitting, using Level 2.0 data from the Beijing station. Figure 3 displays the de-seasonalized time series with 12 month running mean, results of MK test and Sen's slope and linear trend from least squares fitting for the six parameters. According to Fig. 3, three of the parameters, ABS, SSA and AAE exhibit statistically significant (> 90 % and the same hereafter) trends, from both MK and least squares fitting results, while the other parameters do not have significant trends. For ABS, even with a large gap in the time series from 2007 to 2009, a continuous decrease can still be observed from the smoothed time series (black curve in the top panel). The MK test and least squares fitting results are also consistent in indicating significant negative trends. Similarly, consistent increasing trends are found for SSA. Since AOD and SCT do not have significant trends, the decrease in ABS is responsible for the increase in SSA at Beijing. The AAE parameter also shows an increase, although the increase mostly lies in the later part of the time series. Since the mixing of black carbon with other species such as dust and organic carbon tends to increase the AAE value (Russell et al., 2010), this result may imply a reduction in black carbon fraction, which is consistent with the decrease in ABS and increase in SSA. The normal probability plots (normplots) of the least squares fitting residuals are also presented in Fig. 4, which

ACPD
14, 14351–14397, 2014

shows that the residuals follow a normal distribution and thus verifies the validity of least squares fitting.

3.4 Trend comparison between Level 1.5 and Level 2.0 data

As Level 1.5 data have larger uncertainties and more outliers compared to Level 2.0 data, it is possible that these problems may lead to the uncertainty of the trends. On the other hand, since Level 2.0 data sampling is constrained to high AOD conditions, the lack of samples at low AOD conditions may bias the trend estimation. Therefore, here we briefly compare the trends estimated using both data levels for the Beijing station. Figure 5 shows the time series and trends using Level 1.5 data at Beijing. Compared to Fig. 3, we can see that most of the trends between Level 1.5 and Level 2.0 data are consistent, i.e., significant trends for ABS and SSA, and insignificant trends for AOD, SCT and AE are found in both data sets. The only exception is the MK result for the AAE, where Level 2.0 data indicates a significant upward trend while Level 1.5 data does not have a significant trend. As can be seen from the upper panel, the AAE time series itself is not very consistent before and after the 2007–2009 gap, which may have influenced the accuracy of the trend detection. The comparison for the other three stations with sufficient data at both Level 2.0 and Level 1.5, namely IER_Cinzana, Kanpur and XiangHe, also reveals largely consistent trends between these two data levels. The figures are not shown in the main text but are provided in the Supplement. We therefore consider that data level is not a significant factor in affecting the accuracy of the trend analysis.

4 Results

In this section, we focus on presenting and discussing global maps showing the magnitude and significance of the trends of the six variables at each station in the main text, while the plots of the trend analysis at each individual station are included in the

ACPD
14, 14351–14397, 2014

Supplement. Only statistically significant trends (> 90 %) are indicated in the figures. In addition, Table 1 lists the magnitude and significance of the trends at all stations from the MK and least squares analysis. The magnitude is shown as the Sen's slope while the results of least squares fitting is indicated as positive or negative. This is due to the fact that least squares fitting is performed on the logarithm of some parameters so that the magnitude of the trends is not directly comparable to the Sen's slope. Comparing the results for MK and least squares fitting, we see that the two techniques yield consistent results in the significance for the majority of the cases. In the following discussion, we only present trends that are determined to be significant by both methods as we consider these are the trends to be the most robust.

4.1 AOD and SCT trends

Statistically significant AOD and SCT trends at 440 nm at the selected stations are presented in Figs. 6 and 7, respectively. The distribution of the trends for these parameters are quite alike, which is reasonable as scattering aerosols, such as sulfates and nitrates, constitute a large fraction of total aerosol loading. The majority of the stations with significant trends exhibit negative trends in both AOD and SCT, including most stations in North America, Europe, one biomass burning site in South America (CUIABA-MIRANDA) and one urban site in Japan (Osaka). The largest decreases are found over West Europe, which reach –0.1 decade^{-1}. The only exception is the Kanpur station, where upward trends as large as 0.1 decade^{-1} are found in AOD and SCT.

We also examine the trend for each season, using the MK and least squares methods on the seasonal mean time series. The results are shown in Figs. 8 and 9. The patterns on each seasonal trend map agrees in general with the global results for both AOD and SCT. Some stations only exhibit significant trends for certain seasons. For example, the European and North American stations mostly show significant decreasing trends for the spring (MAM), summer (JJA) and fall (SON). For India, significant trends are found during spring and fall. By further examining the time series (figures in the Supplement), it is found that the seasons without significant trends usually have frequent missing

Discussion Paper | Discussion Paper | Discussion Paper | Discussion Paper |
ACPD
14, 14351–14397, 2014
Recent trends in aerosol optical properties derived from AERONET measurements
J. Li et al.

data, which affects or even precludes the detection of trends. Overall, the similarity between the four panels in Figs. 8 and 9, and between Figs. 8 and 9 and 6 and 7 respectively indicate no obvious seasonality in the AOD and SCT trends.

4.2 ABS and SSA trends

Absorption optical depth and single scattering albedo are closely related and both indicate the absorption properties of aerosols. We therefore examine them together. These two parameters play even more important roles in aerosol forcing, as the changes in ABS or SSA not only alter direct forcing, but also have potential impact on aerosol-cloud interaction if the changes are associate with aerosol composition change such as trends in black carbon fraction.

Figure 10 shows global decadal trends for ABS. Significant reduction in aerosol absorption is found at most stations in the Northern Hemisphere, including North America, Europe and East Asia. In particular, three East Asian stations (two in China and one in Japan) all have large decreases in ABS, up to $-0.03\,\text{decade}^{-1}$. East China has been considered as a region of increased aerosol loading in previous studies (e.g., Wang et al., 2009; Zhang and Reid, 2010; Hsu et al., 2012), here AERONET data indicates that ABS has actually declined over the past decade for at least two locations. Nonetheless, because these two stations are both urban sites located in Beijing and Hong Kong, respectively, their ability to represent larger-scale patterns may be limited. Positive ABS trends are found for one site in West Africa (Agoufou), one site in the Arabian Peninsula (Nes_Ziona), a few sites over Western Europe, one site in South America (Campo_Grande_SONDA) and one site in central Australia (Birdsville). Seasonal trends in ABS (Fig. 11) generally show the same pattern and suggest weak seasonality in the trends.

With the overall decrease in ABS revealed by Fig. 10, we expect increases in SSA for most stations. This is indeed the case as shown in Fig. 12. The stations previously indicated to exhibit negative ABS trends mostly have positive SSA trends. Note that the observed SSA trends may be attributed to changes in SCT, ABS or both, and that the reason differs from region to region. For North America, Central and Eastern Europe and Japan, SCT and ABS both decreased with a larger decrease in ABS, resulting in a reduced fraction of absorbing aerosols. For East China, no significant trend is found in SCT while ABS decreased significantly, which also leads to the reduction of absorbing aerosol fraction and consequently an upward SSA trend. For India, however, the increase in SSA is attributed to increases in scattering aerosol fraction (Fig. 7) only with no significant trend in ABS.

The stations with positive ABS trends, mainly for Western Europe, West Africa, South America and central Australia, have negative SSA trends correspondingly. The reduction in SSA is particularly strong for several Western European sites, which is due to both the reduction in SCT and increase in ABS. For stations in South America, West Africa and Australia, since no significant SCT trends are found, the increase in ABS is solely responsible for the reduction in SSA. With respect to seasonal trends (Fig. 13), the distribution of the trends also largely agrees with that of annual results (Fig. 12). Although the magnitude may be different, the signs of the trend are consistent for all stations. Many stations only exhibit trends for one or two seasons. This is primarily due to the lack of sufficient data for some seasons, since we require at least six years of data for each season in order to estimate the trend.

4.3 AE trends

The Ångström Exponent parameter is an indication of the contribution of fine and coarse mode aerosols and can also be potentially useful to infer aerosol composition. Globally, the stations with significant AE trends are much fewer than those with AOD, ABS and SSA trends. Also, compared with the time series of the previous three parameters, the time series for AE appears generally noisier, which might be due to the fact that variability in the AOD of each wavelength becomes enlarged in the calculation of the AE. Therefore, we focus on stations that have significant trends in both annual and seasonal results. The annual and seasonal trend maps are presented in Figs. 14 and 15.

ACPD
14, 14351–14397, 2014

Downward trends are found for six European stations and one in Arabian Peninsula (Nes_Ziona). These locations, especially those close to the Mediterranean, are periodically influenced by dust transported from the Sahara and Arabian Peninsula (Barkan et al., 2005; Klein et al., 2010; Gkikas et al., 2013). The decrease in the AE suggests an increase in coarse mode fraction. Combining the previous decreasing trends found in AOD and SCT, the trend in the AE is likely the result of reduced anthropogenic aerosol emission for Europe. Two other European stations close to North Africa show positive AE trends, as these two stations are primarily affected by dust transported from the Sahara and AOD and ABS both decreased for these two stations (see Figs. 6 and 10), the AE trends are likely associated with decreased dust loading. The seasonality of the European trends supports the above hypothesis. The negative trends are mainly found in the summer months (JJA), when the loading of anthropogenic aerosols reaches maximum, while the positive trends are mostly found in the spring, when the contribution of dust aerosols from the Sahara is highest (Barnaba and Gobbi, 2004). One station in South America (Campo_Grande_SONDA) also shows a negative AE trend, which is significant during summer and fall seasons. This station is located in a rural region of Brazil and is primarily affected by biomass burning aerosols during these two seasons. Recall that Figs. 7 and 10 suggest this station has decreasing SCT trend but increasing ABS trend, therefore the decrease of AE is likely due to the decrease of fine mode scattering species rather than black carbon. Although trends are also found for several other locations, their annual and seasonal trends are not consistent, which are most likely result from high variability or insufficient sampling. We therefore omit the discussion of these sites here.

4.4 AAE trends

The Absorption Ångström Exponent is proposed as an indicator of aerosol composition (e.g., Russell et al., 2010), and is determined by the mixing of different absorbing species including black carbon, dust and organic carbon aerosols. The AAE is defined

ACPD
14, 14351–14397, 2014

as

$$\mathrm{AAE} = \log(\mathrm{ABS}_{\lambda_1}/\mathrm{ABS}_{\lambda_2})/\log(\lambda_1/\lambda_2) \tag{8}$$

where ABS_{λ_1} and ABS_{λ_2} are aerosol absorption optical depth at two wavelengths λ_1 and λ_2, respectively. The theoretical value of AAE for black carbon is 1, and the value increases in the presence of dust and organic carbon. This parameter is considered here because we hope to infer information on the change in aerosol composition associated with the trends in ABS and SSA, e.g., to examine whether the change of black carbon is responsible for the observed SSA or ABS trends. However, similar to the AE, the AAE time series also appears noisier since variability of ABS at each wavelength propagates to the logarithm of the ratio. As a result, we only briefly discuss representative stations that indicate significant trends in both annual and seasonal results.

The annual and seasonal trends for AAE are shown in Figs. 16 and 17. It is found that many of the stations that have negative ABS/positive SSA trends, including Beijing, Central Europe and Northeast America, also display increasing AAE trends. This result is consistent with our expectation that decrease in ABS is associated with decreased black carbon fraction. However, there are also several stations where the changes in AAE are not consistent with changes in ABS and SSA. For example, a negative AAE trend is found for Kanpur (India), while this station has positive SCT trend but no ABS trend, according to which we would expect no significant change or increase in the AAE. Also, the Osaka station in Japan has negative AAE trends possibly indicating increased black carbon fraction, while the SSA at this station also experienced an increase. Moreover, a few stations with significant SSA trends do not appear to have significant AAE trends. Difficulties in interpreting the AAE parameter also confound understanding the results. This parameter depends on the interaction of several aerosol species, which frequently produce intermediate values that may be ambiguous. Therefore, more information, such as that from in-situ measurements of aerosol physical and optical properties, is needed to fully resolve the change in aerosol composition.

To summarize the results, AERONET retrievals from stations with long-term data records reveal significant trends in AOD, SCT, ABS and SSA overall many worldwide

ACPD
14, 14351–14397, 2014

locations. Specifically, Europe and North America experienced a strong decline in total AOD and SCT during the past 13 years. The Kanpur station in Northern India is the only place that exhibits positive AOD and SCT trends. Aerosol absorption has also largely declined over North America and Europe, although a few stations in Western Europe have weak positive ABS trends. Strong negative ABS trends are also found for four stations in East Asia and Northern Australia. Due to the decrease of ABS, SSA shows positive trends for the majority of European, North American and East Asian stations. The Kanpur station also has a positive SSA trend but it is due to the increase of SCT. The stations with significant AE and AAE trends are much fewer and the spatial patterns of the trends are less coherent. The AE trends indicate decreased fine mode fraction over most central Europe, and decreased coarse mode fraction for two sites close to North Africa, and decreased fine mode fraction at one site in South America. The AAE has positive trends for East Asia, Europe and Northeast America, which appears consistent with decreased ABS and suggests a reduced black carbon fraction. However, there still exist considerable inconsistency between the AAE and SSA trends and additional information is needed to determine the change in aerosol composition.

5 Discussion

The significant decline in found in AERONET AOD, SCT and ABS over Europe and North America is consistent with studies using satellite remote sensing products (e.g., Zhang and Reid, 2010; Hsu et al., 2012) and visibility data (Wang et al., 2009), and independent studies using Level 2.0 AERONET direct beam retrievals (Xia et al., 2011; Yoon et al., 2012). The sign of the trends are also in good agreement with trends of aerosol scattering and absorption coefficients derived from in-situ measurements reported by Collaud Coen et al. (2013), although Collaud Coen et al. (2013) suggested stronger decline in scattering coefficients for North America than Europe, and also less significant trends in absorption than scattering, while the AERONET data indicated significant decreases in both scattering and absorption, and comparable trends for North America and Europe. These slightly differences may come from several factors. For example, Collaud Coen et al. (2013) utilizes in-situ sampling at surface while AERONET represent column property. Also, most of the sites in Collaud Coen et al. (2013) are remote sites while many of the selected AERONET stations locate in urban area. The timing of these trends also appears to be inline with emission control measures that have taken place in Europe and North America during the past decades. In the US, $PM_{2.5}$ has been estimated to have been reduced by 50 % and SO_2 by 55 % (EPA, 2011). Murphy et al. (2011) found significant decreases in both $PM_{2.5}$ and elemental carbon using data form the IMPROVE network. Reductions in $PM_{2.5}$ and SO_2 are also reported for Europe (Tørseth et al., 2012), although the decrease is weaker than that found for the US.

The positive SSA trends found over East Asia (East China and Japan) agree with the results of a previous study by Lyapustin et al. (2011) also using AERONET data and with the results of an analysis of independent measurements by Kudo et al. (2010). The reduction of ABS for the China stations, especially Beijing, seems somewhat controversial in light of the trends in emission inventories. For example, Lu et al. (2011) indicated an increase in SO_2 emission in China by 62 % from 2000 to 2006, with a decrease by 9.2 % from 2006 to 2010, while black carbon and organic carbon emissions increased by 72 % and 43 % respectively, from 2000 to 2010. Zhang et al. (2009) also suggested emission growth by 13–55 % from 2001 to 2006 for most species including SO_2 and black carbon. The results presented here are only from two stations: Beijing and Hong_Kong_PolyU. Both are urban stations and might not be representative of surrounding regions. Moreover, the aerosol properties in Beijing are perturbed by the air quality control measures during the Olympic games (e.g., Cermak and Knutti, 2009; Zhang et al., 2009; Guo et al., 2013), which may be one of the reasons of the observed decline in ABS. However, difficulty arises as most of the AERONET stations in China were established in recent years and their records are not long enough for trend analysis, while satellite remote sensing techniques are not capable in retrieving absorption

ACPD
14, 14351–14397, 2014

properties. More information on observation-based trend analysis in China may become possible in the next few years when more of the stations will have longer-term measurements.

The positive AOD trends found at Kanpur, India, is consistent with studies using satellite remote sensing product (Dey and Girolamo, 2011; Ramachandran et al., 2012), and independent ground-based measurements (Babu et al., 2013). The AERONET results presented here imply that scattering aerosols are primarily responsible for this increase in AOD. The increase in aerosol scattering also largely agrees with positive trends in SO_2 over India, as reported by Lu et al. (2013) and Mallik et al. (2013).

Particular attention should be paid to the trend in SSA as revealed by AERONET data. Whether changes in atmospheric aerosol loading will induce a heating or cooling effect on the climate heavily depends on the SSA parameter. It is believed that there is a critical value of the SSA above which aerosols produce a negative forcing (cooling), and below which the aerosol produce a positive forcing (warming). Hansen et al. (1997) concluded from GCM experiments that aerosols with SSA up to 0.9 would lead to global warming, and that the anthropogenic aerosol feedback on the global mean surface temperature is likely to be positive. Ramanathan et al. (2001) indicated that for SSA < 0.95, aerosol net forcing can change from negative to largely positive depending on aerosol height, surface albedo and cloud conditions. Moreover, the change in this parameter implies changes in the relative fraction of absorbing species (mainly black carbon) with respect to scattering aerosols, which may have broad impact on their total radiative effect. Ramana et al. (2010) found that the warming of black carbon strongly depends on the ratio of black carbon to sulfate aerosols. Therefore, the change in SSA for many locations implies a potentially larger change in the aerosol forcing. In particular, while the recent increase in surface radiation, or global brightening, found for Europe, North America and Japan have been largely attributed to the reduction of total aerosol loading, the increase of SSA could also contribute to this trend (Kudo et al., 2010).

ACPD
14, 14351–14397, 2014

Another important consequence of trends in SSA is the impact on satellite retrieved trends of aerosol properties. As most satellite retrieval algorithm assume constant SSA values for the aerosol models, systematic changes in SSA over time may produce spurious tendencies in the retrieved AOD (Mishchenko et al., 2007). Lyapustin et al. (2012) indicated that the temporal change in the bias between MODIS and AERONET AOD over Beijing can be explained by the increase of SSA at this station. Mishchenko et al. (2012) showed that in AVHRR AOD retrieval, decreasing SSA by 0.07 from the start to the end of the data record could eliminate the downward trend in the data. Therefore, the trends in SSA revealed by AERONET measurements should be taken into account in the retrieval algorithms to yield a more accurate representation of temporal changes in aerosol loading.

Admittedly, the AERONET data are not perfect. Several limitations may affect the accuracy of the trend analysis presented here. Although uncertainties in individual measurements largely cancel out in the monthly medians, the accuracy of the trends may still be affected by different sampling frequencies for different months due to variability in meteorological variables such as cloud amount. Another issue is the spatial representativeness of the stations. Many of the stations selected here are urban sites, where aerosol properties tend to be highly variable due to the influence of many local emission sources. For example, some nearby stations in Europe have opposite trends in the ABS and SSA, which suggests that they may be dominated by different local sources and aerosol types. To address this problem, more efforts should be given to maintaining long-term, continuous monitoring of aerosol properties at remote locations. Nonetheless, to date, AERONET is the most extensive ground-based aerosol observation network with high retrieval accuracy, and the trends presented here are significant by both MK test and least squares fitting methods. Both these factors improve the robustness of the results.

ACPD
14, 14351–14397, 2014

6 Conclusions

In this study, we present the results of a trend analysis of key aerosol properties retrieved from AEREONT measurements. Although trends in total aerosol loading such as AOD have been extensively investigated, fewer studies are found for the absorption and scattering properties. This work therefore serves as a reference for evaluating recent changes in aerosol forcing and the assessment of emission inventories and emission control measures. The major conclusions are summarized below:

- Significant decreases in AOD and SCT are found for most locations, in particular, North America and Europe. The Kanpur station in North India experienced increases in AOD and SCT;

- ABS is also found to decrease for North America and most European stations. Two stations in East China, one in Japan and one in North Australia also have negative ABS trends. ABS slightly increased for a few Western European stations. Large positive trends are found for one station in West Africa and one station in South America;

- The decrease in ABS results in an overall increase in SSA for North America, most of Central and Eastern Europe and East Asia. The increase in SCT also leads to an increase in SSA for Kanpur. While the stations with positive ABS trends exhibit declines in SSA;

- No obvious seasonal shifts of the trends are found for the above four parameters;

- Fewer stations show significant AE trends, and the annual and seasonal trends are also less consistent. Several stations in Central Europe exhibit negative trends, indicating decreased fine mode fraction, which may be attributed to the decline in anthropogenic aerosol emissions. A negative trend is also found for one station in Central South America. While positive trends are found for two European stations influenced by Saharan dust transport;

ACPD
14, 14351–14397, 2014

- The AAE parameter also has fewer significant trends. North America, Europe and East Asia appear to have increasing AAE trends, which implies a reduction in black carbon fraction and is consistent with the negative ABS trends at these locations. However, not all AAE and ABS/SSA trends are consistent and more measurements of aerosol composition are likely needed.

The Supplement related to this article is available online at doi:10.5194/acpd-14-14351-2014-supplement.

Acknowledgements. We thank the AERONET team, especially the PIs of the 63 selected stations, for providing the data used in this study. This study is funded by NASA climate grant 509496.02.08.04.24. Jing Li also acknowledges Hal Maring and the NASA Radiation Science program for providing funding for this investigation.

References

Babu, S. S., Manoj, M. R., Moorthy, K. K., Gogoi, M. M., Nair, V. S., Kumar Kompalli, S., Satheesh, S. K., Niranjan, K., Ramagopal, K., Bhuyan, P. K., and Singh, D.: Trends in aerosol optical depth over Indian region: potential causes and impact indicators, J. Geophys. Res.-Atmos., 118, 11794–11806, doi:10.1002/2013JD020507, 2013.

Barkan, J., Alpert, P., Kutiel, H., and Kishcha, P.: Synoptics of dust transportation days from Africa toward Italy and central Europe, J. Geophys. Res., 110, D07208, doi:10.1029/2004JD005222, 2005.

Barnaba, F. and Gobbi, G. P.: Aerosol seasonal variability over the Mediterranean region and relative impact of maritime, continental and Saharan dust particles over the basin from MODIS data in the year 2001, Atmos. Chem. Phys., 4, 2367–2391, doi:10.5194/acp-4-2367-2004, 2004.

Cermak, J. and Knutti, R.: Beijing Olympics as an aerosol field experiment, Geophys. Res. Lett., 36, L10806, doi:10.1029/2009GL038572, 2009.

Charlson, R. J., Schwartz, S. E., Hales, J. M., Cess, R. D., Coakley Jr., J. A., Hansen, J. E., and Hoffman, D. J.: Climate forcing by anthropogenic aerosols, Science, 255, 423–430, doi:10.1126/science.255.5043.423, 1992.

Cheng, T., Chen, H., Gu, X., Yu, T., Guo, J., and Guo, H.: The inter-comparison of MODIS, MISR and GOCART aerosol products against AERONET data over China, J. Quant. Spectrosc. Ra., 113, 2135–2145, 2012.

Christopher, S. A., Gupta, P., Haywood, J., and Greed, G.: Aerosol optical thicknesses over North Africa: 1. Development of a product for model validation using Ozone Monitoring Instrument, Multiangle Imaging Spectroradiometer, and Aerosol Robotic Network, J. Geophys. Res., 113, D00C04, doi:10.1029/2007JD009446, 2008.

Collaud Coen, M., Andrews, E., Asmi, A., Baltensperger, U., Bukowiecki, N., Day, D., Fiebig, M., Fjaeraa, A. M., Flentje, H., Hyvärinen, A., Jefferson, A., Jennings, S. G., Kouvarakis, G., Lihavainen, H., Lund Myhre, C., Malm, W. C., Mihapopoulos, N., Molenar, J. V., O'Dowd, C., Ogren, J. A., Schichtel, B. A., Sheridan, P., Virkkula, A., Weingartner, E., Weller, R., and Laj, P.: Aerosol decadal trends – Part 1: In-situ optical measurements at GAW and IMPROVE stations, Atmos. Chem. Phys., 13, 869–894, doi:10.5194/acp-13-869-2013, 2013.

Dey, S. and Di Girolamo, L.: A decade of change in aerosol properties over the Indian subcontinent, Geophys. Res. Lett., 38, L14811, doi:10.1029/2011GL048153, 2011.

Dubovik, O., Lapyonok, T. V., and Oshchepkov, S. L.: Improved technique for data inversion: optical sizing of multicomponent aerosols, Appl. Optics, 34, 8422–8436, 1995.

Dubovik, O. and King, M. D.: A flexible inversion algorithm for retrieval of aerosol optical properties from Sun and sky radiance measurements, J. Geophys. Res., 105, 20673–20696, 2000.

Dubovik, O., Smirnov, A., Holben, B. N., King, M. D., Kaufman, Y. J., Eck, T. F., and Slutsker, I.: Accuracy assessments of aerosol optical properties retrieved from AERONET Sun and sky-radiance measurements, J. Geophys. Res., 105, 9791–9806, 2000.

Dubovik, O., Holben, B. N., Eck, T. F., Smirnov, A., Kaufman, Y. J., King, M. D., Tanré, D., and Slutsker, I.: Variability of absorption and optical properties of key aerosol types observed in worldwide locations, J. Atmos. Sci., 59, 590–608, 2002.

Dubovik, O., Sinyuk, A., Lapyonok, T., Holben, B. N., Mishchenko, M., Yang, P., Eck, T. F., Volten, H., Munoz, O., Veihelmann, B., van der Zander, W. J., Sorokin, M., and Slutsker, I.: Application of light scattering by spheroids for accounting for particle non-sphericity in remote sensing of desert dust, J. Geophys. Res., 111, D11208, doi:10.1029/2005JD006619, 2006.

Edie, W. T., Dryard, D., James, F. E., Roos, M., and Sadoulet, B.: Statistical Methods in Experimental Physics, North-Holland Publishing Company, Amsterdam, 155 pp., 1971.
EPA: Emissions of primary particulate matter and secondary particulate matter precursors, Assessment published December 2011, available at: http://www.epa.gov/ttn/chief/trends/ (last access: February 2014), CSI 003, 2011.
Gkikas, A., Hatzianastassiou, N., Mihalopoulos, N., Katsoulis, V., Kazadzis, S., Pey, J., Querol, X., and Torres, O.: The regime of intense desert dust episodes in the Mediterranean based on contemporary satellite observations and ground measurements, Atmos. Chem. Phys., 13, 12135–12154, doi:10.5194/acp-13-12135-2013, 2013.
Guo, S., Hu, M., Guo, Q., Zhang, X., Schauer, J. J., and Zhang, R.: Quantitative evaluation of emission controls on primary and secondary organic aerosol sources during Beijing 2008 Olympics, Atmos. Chem. Phys., 13, 8303–8314, doi:10.5194/acp-13-8303-2013, 2013.
Hansen, J., Sato, M., and Ruedy, R.: Radiative forcing and climate response, J. Geophys. Res., 102, 6831–6864, doi:10.1029/96JD03436, 1997.
Hirsch, R. M. and Slack, J. R.: A nonparametric trend test for seasonal data with serial dependence, Water Resour. Res., 20, 727–732, doi:10.1029/WR020i006p00727, 1984.
Hirsch, R. M., Slack, J. R., and Smith, R. A.: Techniques of trend analysis for monthly water quality data, Water Resour. Res., 18, 107–121, doi:10.1029/WR018i001p00107, 1982.
Holben, B. N., Eck, T. F., Slutsker, I., Smirnov, A., Sinyuk, A., Schafer, J., Giles, D., and Dubovik, O.: Aeronet's Version 2.0 quality assurance criteria, P. SPIE, 6408, 64080Q doi:10.1117/12.706524, 2006.
Holben, B. N., Eck, T. F., Slutsker, I., Tanré, D., Buis, J. P., Setzer, A., Vermote, E., Reagan, J. A., Kaufman, Y. J., Nakajima, T., Lavenu, F., Jankowiak, I., and Smirnov, A.: AERONET – a federated instrument network and data archive for aerosol characterization, Remote Sens. Environ., 66, 1–16, 1998.
Hsu, N. C., Gautam, R., Sayer, A. M., Bettenhausen, C., Li, C., Jeong, M. J., Tsay, S.-C., and Holben, B. N.: Global and regional trends of aerosol optical depth over land and ocean using SeaWiFS measurements from 1997 to 2010, Atmos. Chem. Phys., 12, 8037–8053, doi:10.5194/acp-12-8037-2012, 2012.
Ignatov, A., Holben, B. N., and Eck, T. F.: The lognormal distribution as a reference for reporting aerosol optical depth statistics; empirical tests using multi-year, multi-site AERONET Sunphotometer data, Geophys. Res. Lett., 27, 3333–3336, 2000.

ACPD
14, 14351–14397, 2014

Intergovernmental Panel on Climate Change (IPCC): Climate Change 2013: The Physical Science Basis, Contribution of Working Group I to the Fifth Assessment Report of the Intergovernmental Panel on Climate Change, Cambridge University Press, Cambridge, UK, New York, NY, USA, 2013.

Kahn, R. A., Gaitley, B. J., Martonchik, J. V., Diner, D. J., Crean, K. A., and Holben, B.: Multiangle Imaging Spectroradiometer (MISR) global aerosol optical depth validation based on 2 years of coincident Aerosol Robotic Network (AERONET) observations, J. Geophys. Res., 110, D10S04, doi:10.1029/2004JD004706, 2005.

Kaufman, Y. J., Dubovik, O., Smirnov, A., and Holben, B. N.: Remote sensing of non-aerosol absorption in cloud free atmosphere, Geophys. Res. Lett., 29, 1857, doi:10.1029/2001GL014399, 2002.

Kendall, M. G.: Rank Correlation Methods, Griffin, London, 1975.

Klein, H., Nickovic, S., Haunold, W., Bundke, U., Nillius, B., Ebert, M., Weinbruch, S., Schuetz, L., Levin, Z., Barrie, L. A., and Bingemer, H.: Saharan dust and ice nuclei over Central Europe, Atmos. Chem. Phys., 10, 10211–10221, doi:10.5194/acp-10-10211-2010, 2010.

Kudo, R., Uchiyama, A., Yamazaki, A., Sakami, T., and Kobayashi, E.: From solar radiation measurements to optical properties: 1998–2008 trends in Japan, Geophys. Res. Lett., 37, L04805, doi:10.1029/2009GL041794, 2010.

Lu, Z., Zhang, Q., and Streets, D. G.: Sulfur dioxide and primary carbonaceous aerosol emissions in China and India, 1996–2010, Atmos. Chem. Phys., 11, 9839–9864, doi:10.5194/acp-11-9839-2011, 2011.

Lu, Z., Streets, D. G., de Foy, B., and Krotkov, N. A.: OMI observations of interannual increase in SO_2 emissions from Indian coal-fired power plants during 2005–2012, Environ. Sci. Technol., 47, 13993–14000, doi:10.1021/es4039648, 2013.

Lyapustin, A., Smirnov, A., Holben, B., Chin, M., Streets, D. G., Lu, Z., Kahn, R., Slutsker, I., Laszlo, I., Kondragunta, S., Tanré, D., Dubovik, O., Goloub, P., Chen, H.-B., Sinyuk, A., Wang, Y., and Korkin, S.: Reduction of aerosol absorption in Beijing since 2007 from MODIS and AERONET, Geophys. Res. Lett., 38, L10803, doi:10.1029/2011GL047306, 2011.

Mahowald, N. M., Ballantine, J. A., Feddema, J., and Ramankutty, N.: Global trends in visibility: implications for dust sources, Atmos. Chem. Phys., 7, 3309–3339, doi:10.5194/acp-7-3309-2007, 2007.

ACPD
14, 14351–14397, 2014

Title Page
Abstract | Introduction
Conclusions | References
Tables | Figures
◂◂ | ▸▸
◂ | ▸
Back | Close
Full Screen / Esc
Printer-friendly Version
Interactive Discussion

Mallet, M., Dubovik, O., Nabat, P., Dulac, F., Kahn, R., Sciare, J., Paronis, D., and Léon, J. F.: Absorption properties of Mediterranean aerosols obtained from multi-year ground-based remote sensing observations, Atmos. Chem. Phys., 13, 9195–9210, doi:10.5194/acp-13-9195-2013, 2013.
Mallik, C., Lal, S., Naja, M., Chand, D., Venkataramani, S., Joshi, H., and Pant, P.: Enhanced SO_2 concentrations observed over northern India: role of long-range transport, Int. J. Remote Sens., 34, 2749–2762, 2013.
Mann, H. B.: Nonparametric tests against trend, Econometrica, 13, 245–259, 1945.
Mishchenko, M. O., Cairns, B., Hansen, J. E., Travis, L. D., Kopp, G., Schueler, C. F., Fafaul, B. A., Hooker, R. J., Maring, H. B., and Itchkawich, T.: Accurate monitoring of terrestrial aerosols and total solar irradiance: introducing the Glory mission, B. Am. Meteorol. Soc., 88, 677–691, 2007.
Mishchenko, M. I., Liu, L., Geogdzhayev, I. V., Li, J., Carlson, B. E., Lacis, A. A., Cairns, B., and Travis, L. D.: Aerosol retrievals from channel-1 and -2 AVHRR radiances: long-term trends updated and revisited, J. Quant. Spectrosc. Ra.,113, 1974–1980, doi:10.1016/j.jqsrt.2012.05.006, 2012.
Murphy, D. M., Chow, J. C., Leibensperger, E. M., Malm, W. C., Pitchford, M., Schichtel, B. A., Watson, J. G., and White, W. H.: Decreases in elemental carbon and fine particle mass in the United States, Atmos. Chem. Phys., 11, 4679–4686, doi:10.5194/acp-11-4679-2011, 2011.
Omar, A. H., Won, J.-G., Winker, D. M., Yoon, S.-C., Dubovik, O., and McCormick, M. P.: Development of global aerosol models using cluster analysis of Aerosol Robotic Network (AERONET) measurements, J. Geophys. Res., 110, D10S14, doi:10.1029/2004JD004874, 2005.
Prasad, A. K. and Singh, R. P.: Changes in aerosol parameters during major dust storm events (2001–2005) over the Indo-Gangetic Plains using AERONET and MODIS data, J. Geophys. Res., 112, D09208, doi:10.1029/2006JD007778, 2007.
Ramana, M. V., Ramanathan, V., Feng, Y., Yoon, S. C., Kim, S. W., Carmichael, G. R., and Schauer, J. J.: Warming influenced by the ratio of black carbon to sulphate and the black-carbon source, Nat. Geosci., 3, 542–545, 2010.
Ramanathan, V., Crutzen, P. J., Kiehl, J. T., and Rosenfeld, D.: Aerosols, climate, and the hydrological cycle, Science, 294, 2119–2124, 2001.
Russell, P. B., Bergstrom, R. W., Shinozuka, Y., Clarke, A. D., DeCarlo, P. F., Jimenez, J. L., Livingston, J. M., Redemann, J., Dubovik, O., and Strawa, A.: Absorption Angstrom Exponent

ACPD
14, 14351–14397, 2014

in AERONET and related data as an indicator of aerosol composition, Atmos. Chem. Phys., 10, 1155–1169, doi:10.5194/acp-10-1155-2010, 2010.
Remer, L. A., Kaufman, Y. J., Tanré, D., Mattoo, S., Chu, D. A., Martins, J. V., Li, R.-R., Ichoku, C., Levy, R. C., Kleidman, R. G., Eck, T. F., Vermote, E., and Holben, B. N.: The MODIS aerosol algorithm, products, and validation, J. Atmos. Sci., 62, 947–973, 2005.
Sen, P. K.: Estimates of the regression coefficient based on Kendall's tau, J. Am. Stat. Assoc., 63, 1379–1389, 1968.
Smirnov, A., Holben, B. N., Eck, T. F., Dubovik, O., and Slutsker, I.: Cloud-screening and quality control algorithms for the AERONET databasem, Remote Sens. Environ., 73, 337–349, 2000.
Stjern, C. W., Stohl, A., and Kristjansson, J. E.: Have aerosols affected trends in visibility and precipitation in Europe?, J. Geophys. Res., 116, D02212, doi:10.1029/2010JD014603, 2011.
Tarantola, A.: Inverse Problem Theory: Methods for Data Fitting and Model Parameter Estimation, Elsevier, Amsterdam, 500 pp., 1987.
Tørseth, K., Aas, W., Breivik, K., Fjæraa, A. M., Fiebig, M., Hjellbrekke, A. G., Lund Myhre, C., Solberg, S., and Yttri, K. E.: Introduction to the European Monitoring and Evaluation Programme (EMEP) and observed atmospheric composition change during 1972–2009, Atmos. Chem. Phys., 12, 5447–5481, doi:10.5194/acp-12-5447-2012, 2012.
von Storch, V H.: Misuses of statistical analysis in climate research, in: Analysis of Climate Variability: Applications of Statistical Techniques, edited by: von Storch, H. and Navarra, A., Springer-Verlag, Berlin, 11–26, 1995
Wang, K., Dickinson, R. E., and Liang, S.: Clear sky visibility has decreased over land globally from 1973 to 2007, Science, 323, 1468–1470, 2009.
Wang, X. L. and Swail, V. R.: Changes of extreme wave heights in Northern Hemisphere oceans and related atmospheric circulation regimes, J. Climate, 14, 2204–2221, 2001.
Weatherhead, E. C., Reinsel, G. C., Tiao, G. C., Meng, X.-L., Choi, D., Cheang, W.-K., Keller, T., DeLuisi, J., Wuebbles, D. J., Kerr, J. B., Miller, A. J., Oltmans, S. J., and Frederick, J. E.: Factors affecting the detection of trends: statistical considerations and applications to environmental data, J. Geophys. Res., 103, 17149–17161, doi:10.1029/98JD00995, 1998.
Wild, M.: Global dimming and brightening: a review, J. Geophys. Res., 114, D00D16, doi:10.1029/2008JD011470, 2009.
Wild, M.: Enlightening global dimming and brightening, B. Am. Meteorol. Soc., 93, 27–37, doi:10.1175/BAMS-D-11-00074.1, 2012.

Wild, M., Gilgen, H., Roesch, A., Ohmura, A., Long, C. N., Dutton, E. G., Forgan, B., Kallis, A., Russak, V., and Tsvetkov, A.: From dimming to brightening: decadal changes in solar radiation at Earth's surface, Science, 308, 847–850, 2005.

Xia, X. G.: Variability of aerosol optical depth and Ångström wavelength exponent derived from AERONET observations in recent decades, Environ. Res. Lett., 6, 044011, doi:10.1088/1748-9326/6/4/044011, 2011.

Yoon, J., von Hoyningen-Huene, W., Kokhanovsky, A. A., Vountas, M., and Burrows, J. P.: Trend analysis of aerosol optical thickness and Ångström exponent derived from the global AERONET spectral observations, Atmos. Meas. Tech., 5, 1271–1299, doi:10.5194/amt-5-1271-2012, 2012.

Yue, S., Pilon, P., Phinney, B., and Cavadias, G.: The influence of autocorrelation on the ability to detect trend in hydrological series, Hydrol. Process., 16, 1807–1829, doi:10.1002/hyp.1095, 2002.

Zhang, J. and Reid, J. S.: A decadal regional and global trend analysis of the aerosol optical depth using a data-assimilation grade over-water MODIS and Level 2 MISR aerosol products, Atmos. Chem. Phys., 10, 10949–10963, doi:10.5194/acp-10-10949-2010, 2010.

Zhang, X. and Zwiers, F. W.: Comment on "Applicability of prewhitening to eliminate the influence of serial correlation on the Mann-Kendall test" by Sheng Yue and Chun Yuan Wang, Water Resour. Res., 40, W03805, doi:10.1029/2003WR002073, 2004.

Zhang, X. Y., Wang, Y. Q., Lin, W. L., Zhang, Y. M., Zhang, X. C., Zhao, P., Yang, Y. Q., Wang, J. Z., Hou, Q., Che, H. Z., Guo, J. P., Li, Y., Gong, S., and Zhang, X. L.: Changes of Atmospheric composition and optical properties over Beijing 2008 Olympic monitoring campaign, B. Am. Meteorol. Soc., 90, 1633–1651, 2009.

ACPD
14, 14351–14397, 2014

Table 1. Location, aerosol type, number of months used in the analysis (N) and 440 nm AOD, SSA and ABS trends at the 63 selected stations. Bold values indicate trends at 90 % significance level. As least squares are performed on the logarithm of some parameters, the trends are only indicated by positive or negative.

Station	Longitude	Latitude	N	Mann–Kendall Trend (decade^{-1}) AOD	ABS	SCT	SSA	AAE	Least Squares Fitting Trend AOD	ABS	SCT	SSA	AAE
North America													
BSRN_BAO_Boulder	−105.0	40.0	140	**−0.02**	**−0.01**	**−0.01**	**0.07**	**0.07**	Positive	**Negative**	Positive	**Positive**	**Positive**
Billerica	−71.3	42.5	107	−0.01	**−0.00**	−0.01	**0.04**	**0.12**	Positive	**Negative**	Positive	Positive	**Positive**
CCNY	−73.9	40.8	114	**−0.03**	**−0.01**	−0.01	**0.12**	−0.00	**Negative**	**Negative**	**Negative**	**Positive**	Positive
Fresno	−119.8	36.8	101	**−0.05**	−0.00	**−0.04**	**−0.03**	−0.04	**Negative**	Positive	**Negative**	Positive	Positive
Halifax	−63.6	44.6	132	−0.00	−0.00	−0.00	0.00	**0.05**	Positive	Positive	Positive	Positive	Positive
KONZA_EDC	−96.6	39.1	124	0.00	**0.00**	−0.00	**0.02**	**−0.08**	Positive	**Positive**	Positive	**Negative**	**Negative**
Maricopa	−112.0	33.1	95	−0.00	**0.01**	−0.01	**−0.08**	**−0.24**	Positive	**Positive**	Positive	**Negative**	**Negative**
Ragged_Point	−59.4	13.2	73	0.05	0.00	**0.04**	0.01	0.09	Positive	Positive	Positive	Positive	Positive
Railroad_Valley	−116.0	38.5	141	**−0.01**	**−0.00**	−0.01	**0.09**	**0.24**	**Negative**	**Negative**	Positive	**Positive**	**Positive**
Thompso_Farm	−70.9	43.1	70	**−0.13**	**−0.01**	**−0.08**	**0.15**	**0.31**	**Negative**	**Negative**	**Negative**	**Positive**	**Positive**
Univ_of_Houston	−95.3	29.7	80	−0.02	**−0.01**	−0.00	**0.07**	−0.00	**Negative**	**Negative**	**Negative**	**Positive**	Positive
White_Sands_HELSTF	−106.3	32.6	83	**0.02**	0.00	**0.02**	0.03	−0.01	Positive	Positive	Positive	Positive	Positive
South America													
Campo_Grande_SONDA	−54.5	−20.4	83	0.02	**0.01**	−0.01	**−0.17**	**−0.24**	Positive	**Positive**	Positive	**Negative**	**Negative**
CEILAP-RG	−69.3	−51.6	90	**−0.01**	**−0.01**	−0.00	**0.19**	0.02	Positive	Positive	Positive	**Positive**	Positive
CUIABA-MIRANDA	−56.0	−15.7	118	**−0.01**	**−0.02**	**−0.05**	**0.11**	0.05	**Negative**	**Negative**	**Negative**	**Positive**	**Positive**
La_Parguera	−67.0	18.0	137	−0.01	**−0.00**	−0.01	**0.02**	**0.06**	Positive	**Negative**	Positive	Positive	Positive
Trelew	−65.3	−43.3	95	**0.01**	**0.01**	0.00	**−0.19**	**0.18**	**Positive**	**Positive**	Positive	**Negative**	Positive
Europe													
Barcelona	2.1	41.4	104	**−0.09**	**−0.01**	**−0.07**	**−0.04**	−0.04	**Negative**	**Negative**	**Negative**	**Positive**	**Positive**
Belsk	20.8	51.8	111	**−0.05**	0.00	**−0.04**	**−0.03**	**−0.11**	**Negative**	Positive	**Negative**	Positive	**Negative**
Burjassot	−0.4	39.5	73	**−0.06**	**0.01**	**−0.07**	**−0.15**	**−0.12**	**Negative**	**Positive**	**Negative**	**Negative**	**Negative**
Cabauw	4.9	52.0	100	**−0.09**	**−0.01**	**−0.09**	**0.04**	−0.05	**Negative**	**Negative**	**Negative**	Positive	Positive
Cabo_da_Roca	−9.5	38.8	86	−0.02	**0.01**	**−0.03**	**−0.07**	0.04	Positive	**Positive**	**Negative**	**Negative**	Positive
Caceres	−6.3	39.5	80	−0.03	**0.01**	−0.04	**−0.15**	**0.23**	**Negative**	Positive	**Negative**	Positive	**Positive**
Carpentras	5.1	44.1	129	**−0.09**	**−0.01**	**−0.06**	**0.03**	−0.03	**Negative**	**Negative**	**Negative**	**Positive**	Positive
Dunkerque	2.4	51.0	110	**−0.10**	**−0.02**	**−0.07**	**0.16**	**0.18**	**Negative**	**Negative**	**Negative**	**Positive**	Positive
El_Arenosillo	−6.7	37.1	120	**−0.03**	**−0.01**	**−0.02**	**0.05**	0.07	**Negative**	**Negative**	Positive	**Positive**	Positive
Evora	−7.9	38.6	116	**−0.05**	0.00	**−0.05**	**−0.06**	0.01	**Negative**	Positive	**Negative**	**Negative**	Positive
FORTH_CRETE	25.3	35.3	101	−0.02	0.00	**−0.03**	**−0.02**	**−0.13**	Positive	Positive	Positive	**Negative**	**Negative**
Granada	−3.6	37.2	94	**−0.02**	0.00	−0.02	**−0.04**	−0.08	Positive	Positive	**Negative**	**Negative**	**Negative**
IFT-Leipzig	12.4	51.3	119	**−0.07**	−0.00	**−0.07**	0.00	**−0.29**	**Negative**	Positive	**Negative**	Positive	**Negative**
Le_Fauga	1.3	43.4	80	**−0.07**	**0.01**	**−0.10**	**−0.10**	−0.08	**Negative**	**Positive**	**Negative**	**Negative**	**Negative**
Lecce_University	18.1	40.3	112	**−0.06**	**−0.01**	**−0.05**	**0.02**	−0.03	**Negative**	**Negative**	**Negative**	Positive	Positive
Minsk	27.6	53.9	115	**−0.03**	**−0.01**	−0.02	**0.10**	**0.16**	**Negative**	**Negative**	Positive	**Positive**	**Positive**
Moscow_MSU_MO	37.5	55.7	127	−0.02	−0.00	−0.03	−0.01	0.04	Positive	Positive	Positive	Positive	**Positive**
Munich_University	11.6	48.1	80	−0.00	0.00	−0.02	−0.02	0.06	Positive	Positive	**Negative**	**Negative**	Positive
OHP_OBSERVATOIRE	5.7	43.9	100	−0.00	0.00	−0.01	−0.04	**−0.19**	Positive	Positive	Positive	**Negative**	**Negative**
Palencia	−4.5	42.0	110	**−0.04**	**−0.01**	**−0.03**	**0.05**	**0.11**	**Negative**	Positive	**Negative**	Positive	**Positive**
Paris	2.3	48.9	98	**−0.09**	**−0.01**	**−0.07**	**0.07**	**0.16**	**Negative**	**Negative**	**Negative**	**Positive**	**Positive**
Rome_Tor_Vergata	12.6	41.8	125	**−0.03**	**−0.00**	**−0.03**	**0.03**	0.01	**Negative**	**Negative**	**Negative**	Positive	Positive

ACPD
14, 14351–14397, 2014

Recent trends in aerosol optical properties derived from AERONET measurements

J. Li et al.

Table 1. Continued.

Station	Longitude	Latitude	*N*	Mann–Kendall Trend (decade^{-1}) AOD	ABS	SCT	SSA	AAE	Least Squares Fitting Trend AOD	ABS	SCT	SSA	AAE
Saada	−8.2	31.6	96	**−0.09**	**−0.01**	**−0.07**	**0.03**	−0.08	**Negative**	**Negative**	**Negative**	**Positive**	Positive
Sevastopol	33.5	44.6	92	0.02	0.00	−0.01	**−0.06**	0.09	Positive	**Positive**	Positive	**Negative**	Positive
Toravere	26.5	58.3	112	**−0.04**	**−0.01**	0.02	**0.15**	−0.03	Positive	**Negative**	Positive	**Positive**	Positive
Toulon	6.0	43.1	81	−0.05	**−0.01**	−0.04	**0.14**	**−0.08**	Positive	**Negative**	Positive	**Positive**	Positive
Villefranche	7.3	43.7	98	**−0.07**	**−0.01**	**−0.06**	**0.06**	**0.13**	**Negative**	**Negative**	**Negative**	**Positive**	**Positive**
Asia													
Beijing*	116.4	40.0	103	−0.11	**−0.03**	−0.08	**0.04**	**0.32**	Positive	**Negative**	Positive	**Positive**	**Positive**
Kanpur*	80.2	26.5	113	**0.08**	−0.01	**0.07**	**0.03**	**−0.12**	**Positive**	Positive	**Positive**	**Positive**	**Negative**
Hong_Kong_PolyU	114.2	22.3	84	−0.21	**−0.05**	−0.04	**0.18**	**−0.37**	Positive	**Negative**	Positive	**Positive**	**Negative**
Nes_Ziona	34.8	31.9	126	0.00	**0.01**	−0.01	**−0.05**	**−0.10**	Positive	**Positive**	Positive	**Negative**	Positive
Osaka	135.6	34.7	115	**−0.05**	0.00	**−0.06**	−0.01	**−0.10**	**Negative**	Positive	**Negative**	**Negative**	**Negative**
Shirahama	135.4	33.7	135	−0.03	**−0.01**	−0.02	**0.04**	−0.01	Positive	**Negative**	Positive	**Positive**	Positive
Singapore	103.8	1.3	77	0.06	−0.00	0.06	0.03	−0.10	Positive	Positive	Positive	Positive	Positive
XiangHe*	117.0	39.8	113	−0.09	−0.01	−0.06	0.01	0.09	Positive	**Negative**	Positive	Positive	Positive
Africa													
Agoufou	−1.5	15.3	98	0.08	0.01	0.03	−0.01	0.13	Positive	**Positive**	Positive	**Negative**	Positive
Blida	2.9	36.5	86	−0.07	**−0.01**	−0.04	**0.07**	**0.30**	**Negative**	**Negative**	Positive	**Positive**	**Positive**
IER_Cinzana*	−5.9	13.3	97	−0.01	0.00	−0.02	−0.00	**0.58**	Positive	Positive	Positive	Positive	**Positive**
La_Laguna	−16.3	28.5	76	−0.04	0.00	−0.04	−0.05	**0.49**	Positive	Positive	**Negative**	**Negative**	**Positive**
Santa_Cruz_Tenerife	−16.2	28.5	105	**−0.06**	**−0.01**	**−0.04**	**0.07**	**0.07**	**Negative**	**Negative**	**Negative**	**Positive**	Positive
Tamanrasset_INM	5.5	22.8	81	−0.04	**−0.01**	−0.03	**0.07**	0.00	Positive	Positive	Positive	Positive	Positive
Australia													
Birdsville	139.3	−25.9	86	**0.01**	**0.01**	0.00	**−0.20**	−0.07	Positive	**Positive**	Positive	**Negative**	Positive
Canberra	149.1	−35.3	125	−0.00	**0.01**	−0.00	**−0.01**	**−0.06**	Positive	**Positive**	**Negative**	**Negative**	**Negative**
Jabiru	132.9	−12.7	126	0.00	**−0.01**	**0.02**	**0.12**	0.03	Positive	**Negative**	Positive	**Positive**	Positive
Lake_Argyle	128.7	−16.1	124	**0.02**	0.00	0.01	−0.02	0.04	Positive	Positive	Positive	Positive	Positive
Island													
Midway_Island	−177.4	28.2	101	**0.03**	**0.00**	0.01	**−0.06**	−0.01	**Positive**	**Positive**	Positive	**Negative**	Positive

* Level 2.0 data are used for these station.

ACPD
14, 14351–14397, 2014

Recent trends in aerosol optical properties derived from AERONET measurements

J. Li et al.

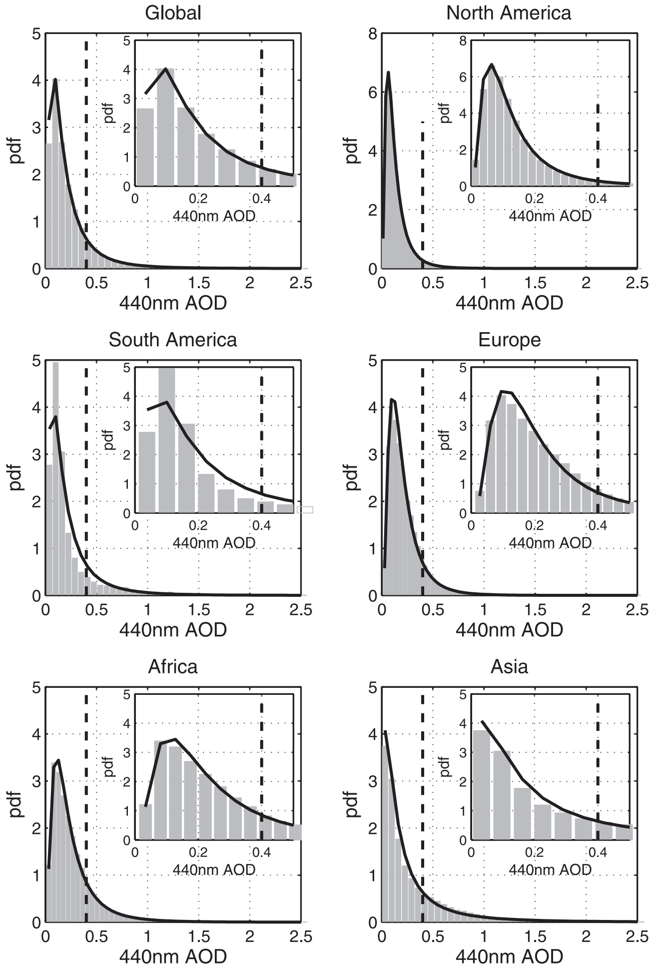

Figure 1. Distribution of AERONET 440 nm AOD for all stations (globe) and stations from five major regions. The data are from the 63 selected stations used for this study as shown in Fig. 2.

ACPD
14, 14351–14397, 2014

Recent trends in aerosol optical properties derived from AERONET measurements

J. Li et al.

Title Page
Abstract | Introduction
Conclusions | References
Tables | Figures
◀| |▶
◀ ▶
Back | Close
Full Screen / Esc
Printer-friendly Version
Interactive Discussion

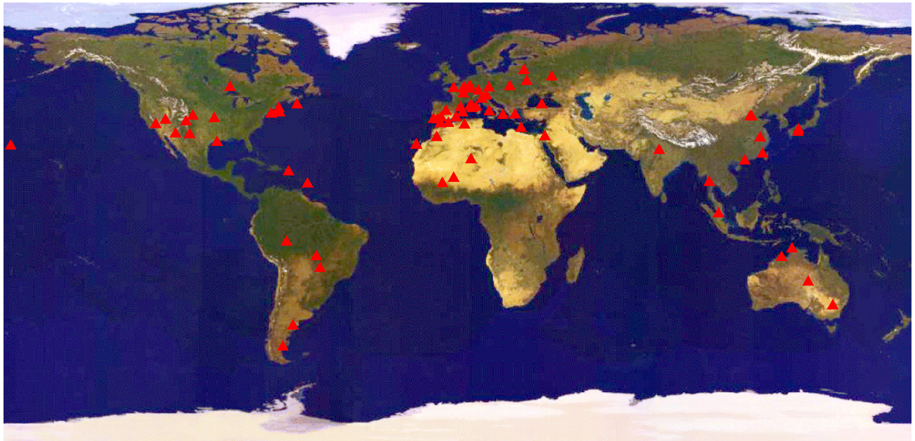

Figure 2. Locations of the stations selected for this study, marked by red triangles.

ACPD
14, 14351–14397, 2014

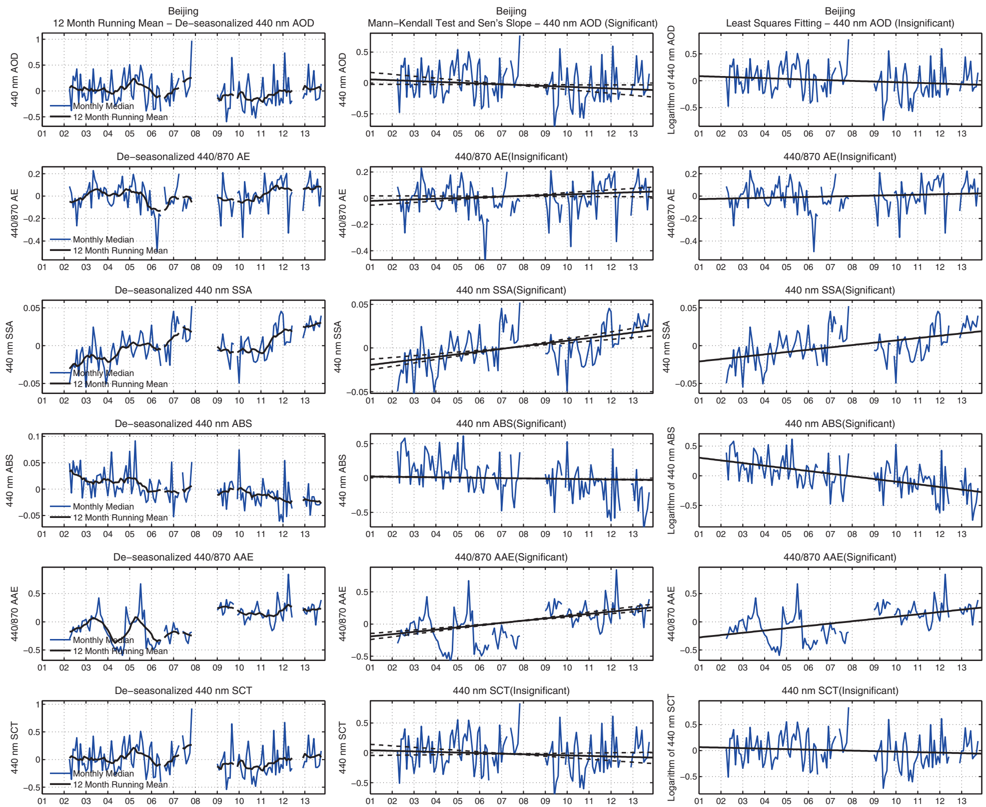

Figure 3. Trend analysis of the six parameters using 12 month running mean (left column), Mann–Kendall test associated with Sen's slope (middle column) and least squares fitting (right column) for Beijing station using Level 2.0 data. The solid black lines in the MK and least squares fitting results show the linear trend, and the dashed curves in the middle column indicates the 90 % confidence interval of the estimated Sen's slope.

ACPD
14, 14351–14397, 2014

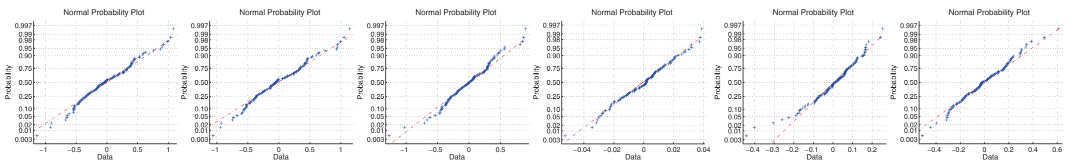

Figure 4. Normplots for the residuals of least square fitting shown in the lower panels of Fig. 2. The majority of the data points concentrate account the red dashed line, indicating that the residuals closely follow a normal distribution.

ACPD
14, 14351–14397, 2014

Recent trends in aerosol optical properties derived from AERONET measurements

J. Li et al.

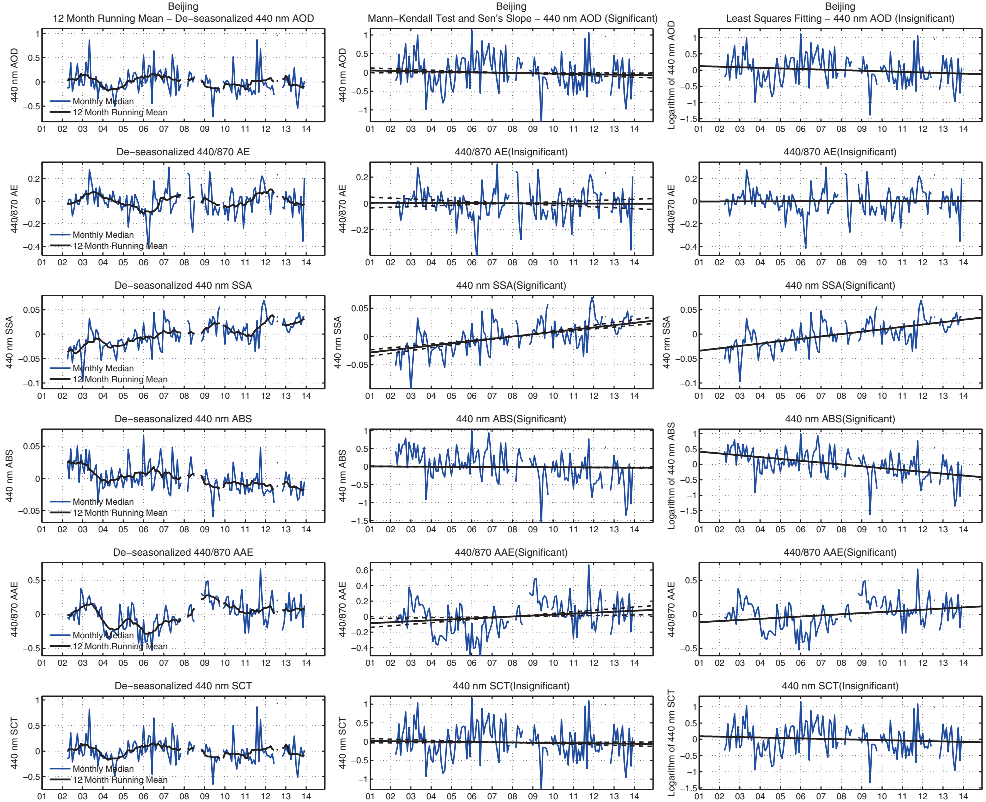

Figure 5. Trend analysis of the six parameters using 12 month running mean (left column), Mann–Kendall test associated with Sen's slope (middle column) and least square fitting (right column) for Beijing station using Level 1.5 data. The black lines in the MK and least squares fitting results show the linear trend, and the dashed curves in the middle panels indicate the 90 % confidence interval of the estimated Sen's slope. Except for the MK test of the AAE, all trends and their significance are consistent with those shown in Fig. 2 calculated using Level 2.0 data.

ACPD
14, 14351–14397, 2014

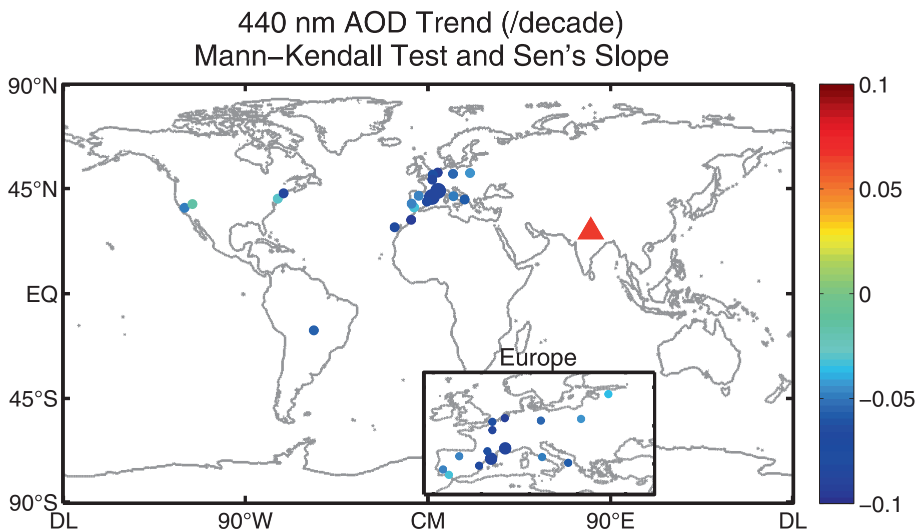

Figure 6. Global map showing the magnitude and significance of the 440 nm AOD trends. Only statistically significant (> 90 %) trends are shown. The triangle indicates Level 2.0 data is used for this station. The smaller dots indicate trends at 90 % significance while larger dots indicate trends at 95 % significance. The magnitude of the trend (decade^{-1}) is indicated by the color of the dots following the color scale on the left. The small panel at the bottom is an enlarged map for Europe.

ACPD
14, 14351–14397, 2014

Recent trends in aerosol optical properties derived from AERONET measurements

J. Li et al.

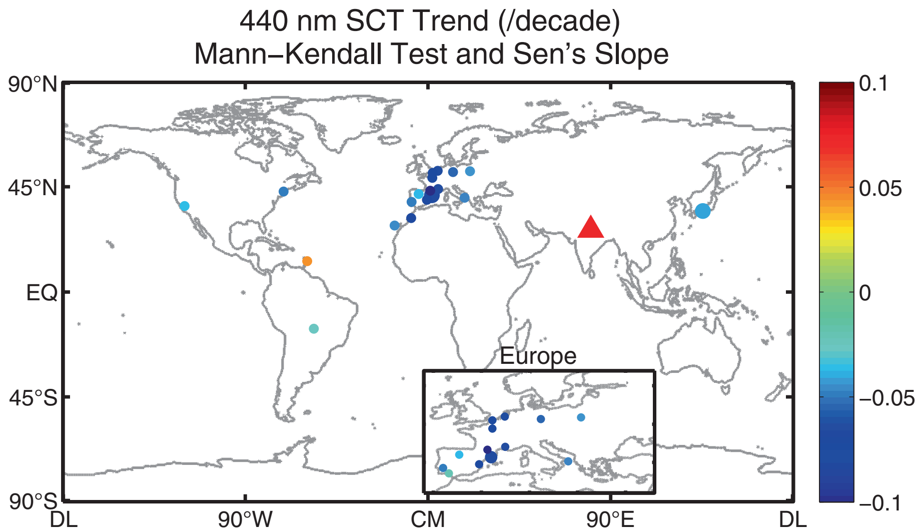

Figure 7. The same as Fig. 5 but for 440 nm SCT Trend.

ACPD
14, 14351–14397, 2014

Recent trends in aerosol optical properties derived from AERONET measurements

J. Li et al.

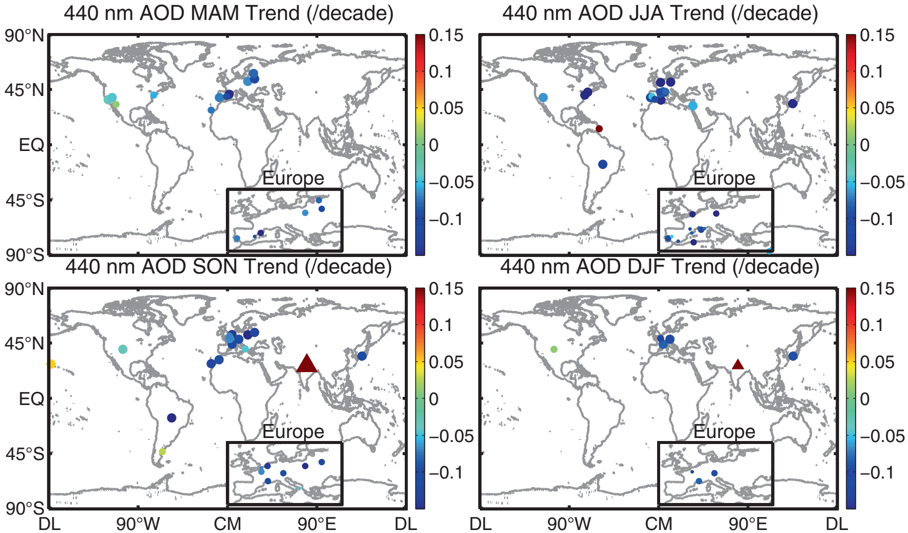

Figure 8. AOD trend maps for the four seasons. Spring (MAM): March-April-May; summer (JJA): June-July-August; fall (SON): September-October-November; winter (DJF): December-January-February.

ACPD
14, 14351–14397, 2014

Recent trends in aerosol optical properties derived from AERONET measurements

J. Li et al.

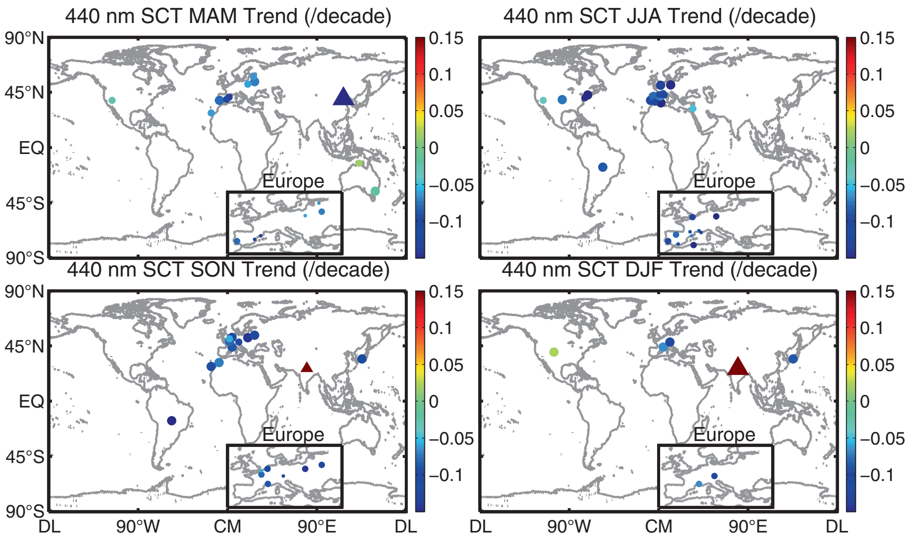

Figure 9. Same as Fig. 7 but for SCT.

ACPD
14, 14351–14397, 2014

Recent trends in aerosol optical properties derived from AERONET measurements

J. Li et al.

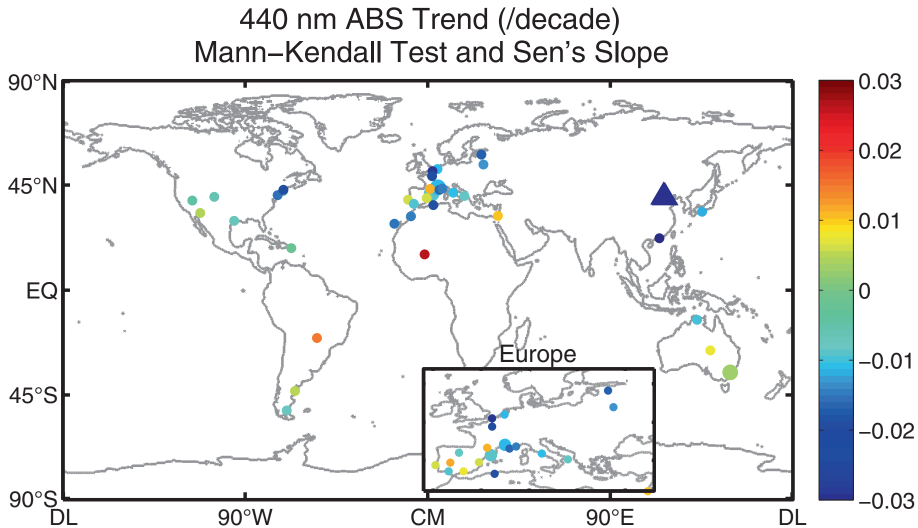

Figure 10. Global map showing the magnitude and significance of the 440 nm ABS trends. Only statistically significant (> 90 %) trends are shown. The triangle indicates Level 2.0 data is used for this station. The smaller dots indicate trends at 90 % significance while larger dots indicate trends at 95 % significance. The magnitude of the trend (decade^{-1}) is indicated by the color of the dots following the color scale on the left. The small panel at the bottom is an enlarged map for Europe.

ACPD
14, 14351–14397, 2014

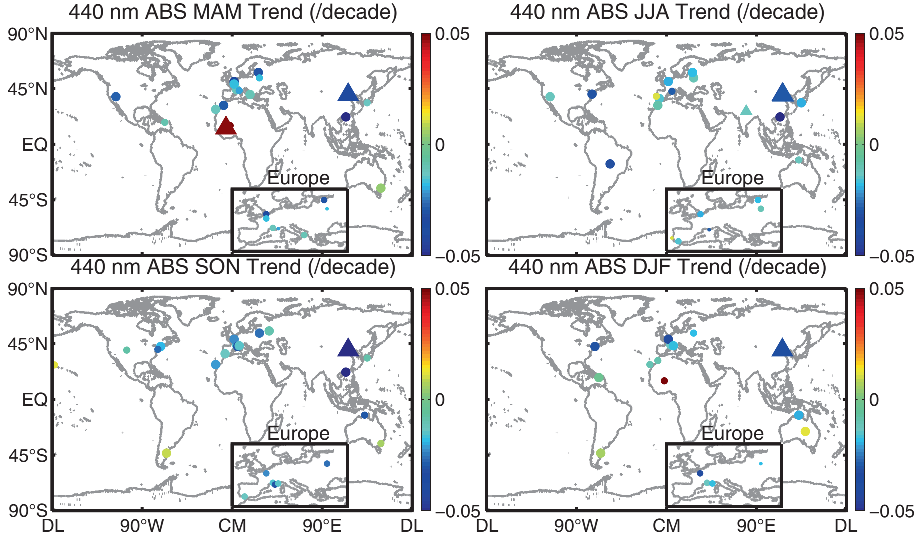

Figure 11. Seasonal trend maps for ABS.

ACPD
14, 14351–14397, 2014

Recent trends in aerosol optical properties derived from AERONET measurements

J. Li et al.

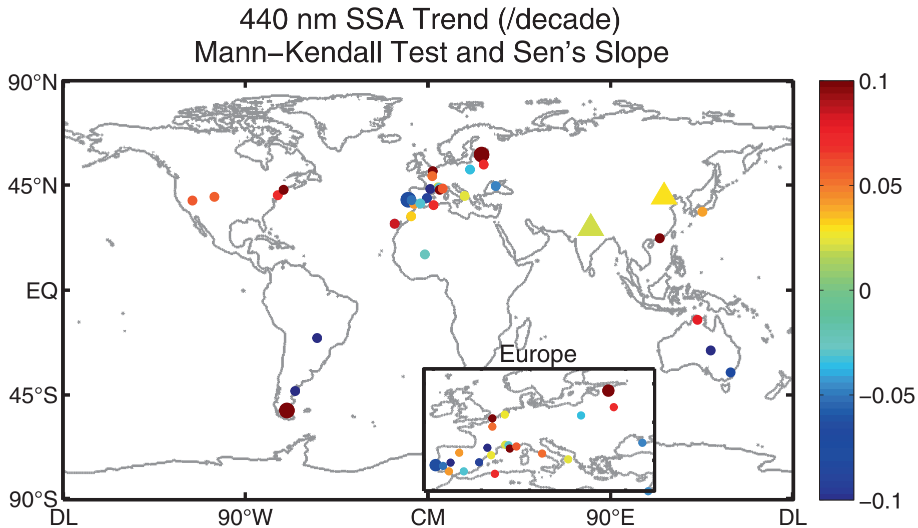

Figure 12. Global map showing the magnitude and significance of the 440 nm SSA trends. Only statistically significant (> 90 %) trends are shown. The triangle indicates Level 2.0 data is used for this station. The smaller dots indicate trends at 90 % significance while larger dots indicate trends at 95 % significance. The magnitude of the trend ($decade^{-1}$) is indicated by the color of the dots following the color scale on the left. The small panels at the bottom is an enlarged map for Europe.

ACPD
14, 14351–14397, 2014

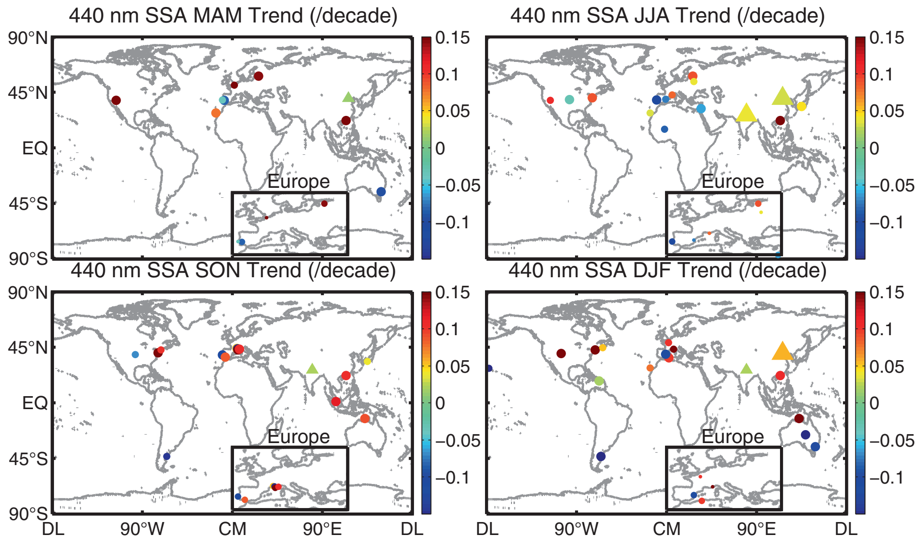

Figure 13. Seasonal trend maps for SSA.

ACPD
14, 14351–14397, 2014

Recent trends in aerosol optical properties derived from AERONET measurements

J. Li et al.

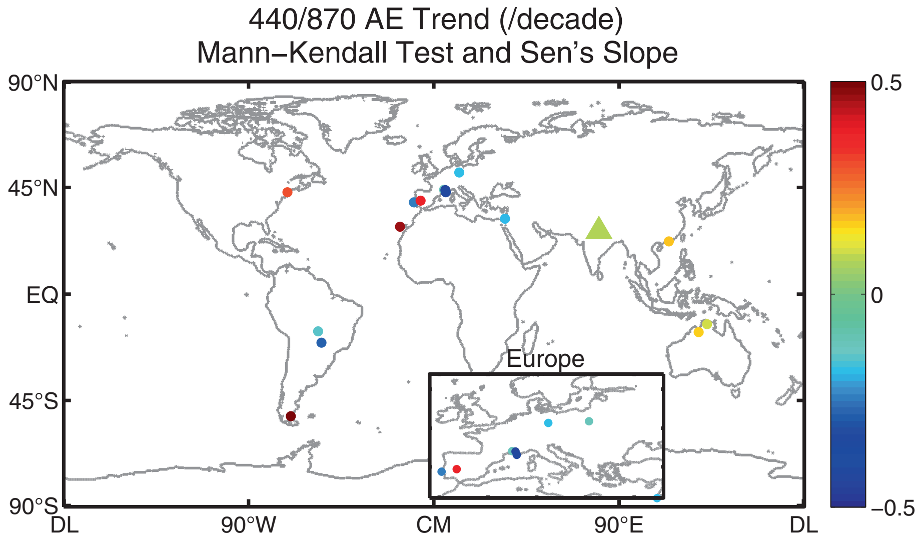

Figure 14. Global map showing the magnitude and significance of the AE trends. The AE is defined using the 440/870 nm AOD pair. Only statistically significant (> 90 %) trends are shown. The triangle indicates that Level 2.0 data is used for this station. The smaller dots indicate trends at 90 % significance while larger dots indicate trends at 95 % significance. The magnitude of the trend ($decade^{-1}$) is indicated by the color of the dots following the color scale on the left. The small panel at the bottom is an enlarged map for Europe.

ACPD
14, 14351–14397, 2014

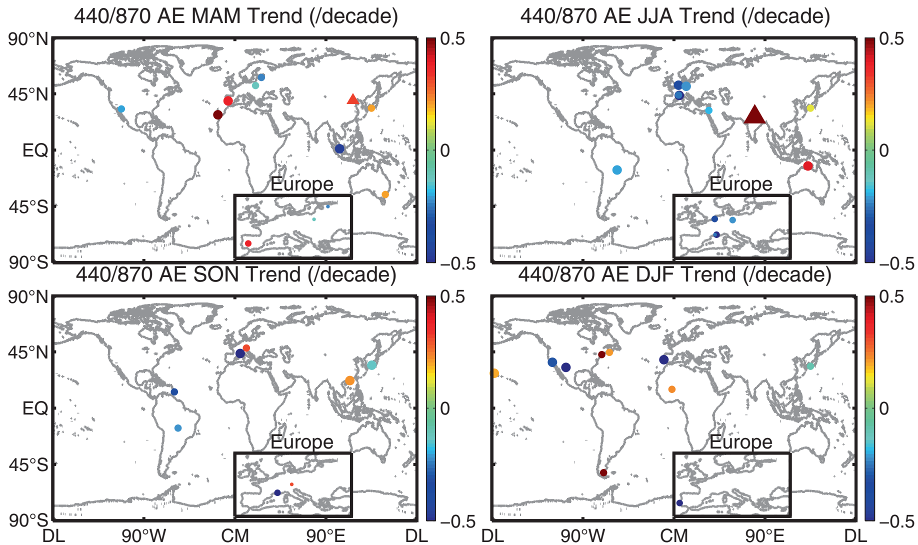

Figure 15. Seasonal trend maps for the AE.

ACPD
14, 14351–14397, 2014

Recent trends in aerosol optical properties derived from AERONET measurements

J. Li et al.

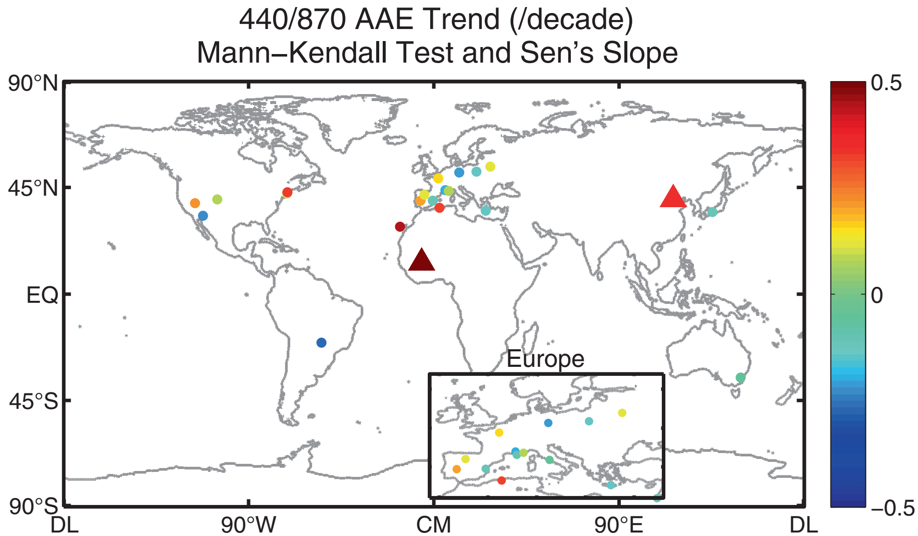

Figure 16. Global map showing the magnitude and significance of the AAE trends. The AEE is defined using the 440/870 nm ABS pair. Only statistically significant (> 90 %) trends are shown. The triangle indicates Level 2.0 data is used for this station. The smaller dots indicate trends at 90 % significance while larger dots indicate trends at 95 % significance. The magnitude of the trend (decade^{-1}) is indicated by the color of the dots following the color scale on the left. The small panel at the bottom is an enlarged map for Europe.

ACPD
14, 14351–14397, 2014

Recent trends in aerosol optical properties derived from AERONET measurements

J. Li et al.

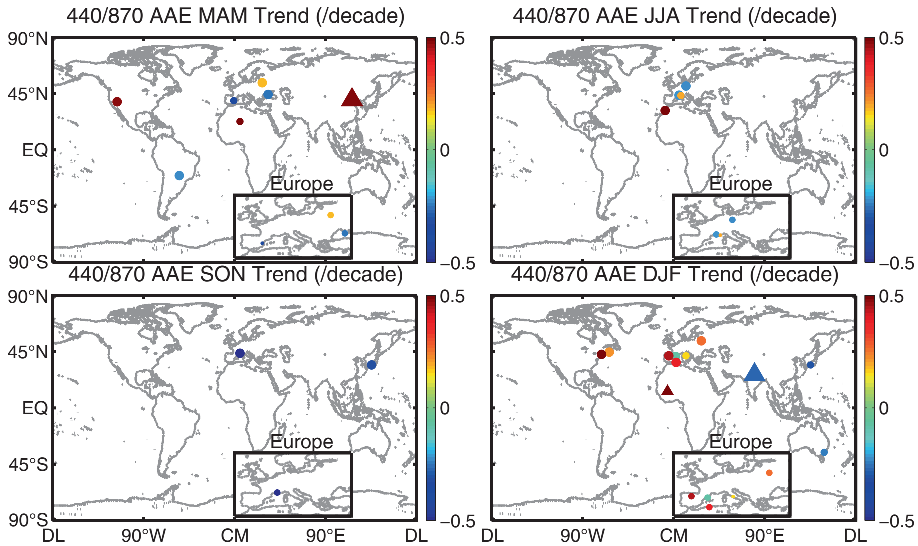

Figure 17. Seasonal trend maps for AAE.

ACPD
14, 14351–14397, 2014

Recent trends in aerosol optical properties derived from AERONET measurements

J. Li et al.